Revista de la Sociedad Química de México, Vol. **46**, *Núm. 2 (2002) 145-158*

Investigación

A comparative *ab initio* Study of the Isomerizations and Hydrolyses of neutral and anionic M-Pyrophosphate Complexes, with M = Ca, Zn

William J. McCarthy,[1] Ludwik Adamowicz,[2] Humberto Saint-Martin[3*] and Iván Ortega-Blake[3]

[1] Biotechnology Center, Utah State University, Logan, Utah 84332, U.S.A.
[2] Department of Chemistry, University of Arizona, Tucson, Arizona 85721, U.S.A.
[3] Centro de Ciencias Físicas, Universidad Nacional Autónoma de México, Apartado Postal 48-3, Cuernavaca, Morelos 62251, México. E-mail: humberto@fis.unam.mx

Recibido el 15 de febrero del 2002; aceptado el 25 de junio del 2002

Abstract. In this work *ab initio* calculations were performed on anhydrous and monohydrated gas-phase calcium and zinc dications chelated with various anionic pyrophosphate species: $H_2P_2O_7^{2-}$, $HP_2O_7^{3-}$ and $P_2O_7^{4-}$. The cleavage of the M-pyrophosphate into a metaphosphate and an orthophosphate coordinated by the dication was also investigated. The studied isomerization reactions were $[M \cdot H_NP_2O_7]^{(2-N)-} \rightarrow [H_NPO_4 \cdot M \cdot PO_3]^{(2-N)-}$ where N = 0, 1, 2, and M = Ca, Zn. These reactions were also studied in the presence of one water molecule and also with a continuum model to mimic the solvation effects. It was found that the interaction with a water molecule stabilizes the pyrophosphates relative to their metaphosphate isomers. Moreover, upon interacting with the dianionic complexes, the water molecule readily breaks and produces a hydroxide anion: $H_2O + [M \cdot P_2O_7]^{2-} \rightarrow [HO \cdot M \cdot HP_2O_7]^{2-}$. The latter dianionic complexes resulted virtually isoenergetic with the hydrolyzed $[M \cdot (HPO_4)_2]^{2-}$ complexes. The results were compared to previous data of magnesium-containing complexes. This comparative analysis shows that the differences in the structures imposed by the various cations may play an important role in the allosteric transformations of the substrate, that ultimately promote the hydrolysis. Though not conclusive, evidence was found that Zn^{2+} has a similar oxidizing power on M-pyrophosphates as Mg^{2+}, whereas the oxidizing power of Ca^{2+} is significantly lower. Nevertheless, the electronic density on the M-pyrophosphates and on the M-phosphates turned out to be very similar for the three cations, and thus the main difference in their biochemical role when interacting with phosphates stems from their different coordination properties, that could even lead to the presence of a hydroxide anion in the first hydration shells of Mg- and Zn-pyrophosphates.
Keywords: Pyrophosphate hydrolysis, metal cations, nucleophilic substitution, coordination properties, *ab initio* calculations.

Resumen. En este trabajo se realizaron cálculos *ab initio* de los dicationes calcio y zinc quelados con varias especies aniónicas de pirofosfato, en la fase gaseosa, anhidros y monohidratados: $H_2P_2O_7^{2-}$, $HP_2O_7^{3-}$ y $P_2O_7^{4-}$. También se investigó la separación del M-pirofosfato en un metafosfato y un ortofosfato coordinados por el dicatión. Se estudiaron las reacciones de isomerización $[M \cdot H_NP_2O_7]^{(2-N)-} \rightarrow [H_NPO_4 \cdot M \cdot PO_3]^{(2-N)-}$ con N = 0, 1, 2, y M = Ca, Zn. Estas reacciones también se estudiaron en presencia de una molécula de agua y también con un modelo continuo para simular los efectos de solvatación. Se encontró que la interacción con una molécula de agua estabiliza los pirofosfatos en relación a sus isómeros con metafosfatos. Además, al interactuar con los complejos dianiónicos, la molécula de agua rápidamente se rompe y produce un anión oxidrilo $H_2O + [M \cdot P_2O_7]^{2-} \rightarrow [HO \cdot M \cdot HP_2O_7]^{2-}$. Estos últimos complejos dianiónicos resultaron virtualmente isoenergéticos con los complejos hidrolizados $[M \cdot (HPO_4)_2]^{2-}$. Se compararon los resultados con datos previos de complejos con magnesio. Este análisis comparativo muestra que las diferencias en las estructuras impuestas por los diversos cationes puede jugar un papel importante en las transformaciones alostéricas del sustrato, que finalmente promueven la hidrólisis. Aunque no concluyente, se encontró evidencia de que Zn^{2+} tiene sobre los M-pirofosfatos un poder oxidativo similar al de Mg^{2+}, en tanto que el poder oxidativo de Ca^{2+} es significativamente menor. Sin embargo, la densidad electrónica en los M-pirofosfatos y en los M-fosfatos resultó ser muy similar para los tres cationes, y entonces la diferencia principal en sus papeles bioquímicos cuando interactúan con fosfatos proviene de sus diferentes propiedades de coordinación, que incluso podrían llevar a la presencia de un anión oxhidrilo en las primeras capas de hidratación de Mg- y Zn-pirofosfatos.
Palabras clave: hidrólisis de pirofosfato, cationes metálicos, sustitución nucleofílica, propiedades de coordinación, cálculos *ab initio*.

Introduction

The concepts of supramolecular chemistry [1] are based on the existence of oligomolecular supermolecules; arrays of components held together by intermolecular forces. These concepts lead to consider the relevance of non-covalent interactions, such as the coordination properties of metal cations, in processes of molecular recognition. As it would be expected, examples of this type of chemistry appear in biochemistry; for instance, in aqueous solution, the forces acting between molecules vary from weak Van der Waals interactions to intermolecular interactions that can hold together assemblies of molecules. Examples of the latter are the hydrogen bond and the coordination properties of ions. The relevance of this type of interaction to the hydrolysis of pyrophosphate was realized three decades ago, when George *et al.* [2] proposed that the free energy of the reaction in solution was due to the difference in hydration energies between reactants and products. Both experimental [3, 4] and theoretical [5-8] studies have been performed to obtain estimates of the hydration energies of pyrophosphate and orthophosphate.

More recent experimental studies [9-13] concluded that the true substrate for pyrophosphatases is the dianionic complex $[Mg \cdot P_2O_7]_2^-$. However, structural data from high reso-

lution X-ray experiments [14] show the presence of four metal cations in the active site of the pyrophosphatase from the budding yeast *Saccharomyces cerevisiae*, leading to propose that the true substrate is the neutral complex [$Mg_2 \cdot P_2O_7$]. This latter species is unlikely to exist in solution under physiological conditions [15], so the question arises of how it can be formed within the active site. At any rate, the species to be studied should be the complexes coordinated by a metal cation. Thus, to answer the question of why Nature chose phosphates for biochemical transformations [16], the coordination properties of the metal cation have to be taken into account. For instance, the experimental characterization of the membrane-bound pyrophosphatase of *Rhodospirillum rubrum* showed that it can utilize zinc complexes as substrates for the hydrolysis of pyrophosphates, with a slightly smaller efficiency, and a distinctly different concentration dependent kinetics, than those for magnesium containing complexes, whereas it cannot utilize calcium complexes for the same purpose [9, 15]. It is also known that the interaction of zinc ions with $CaMgP_2O_7$ granules from cells of the snail *Helix aspersa* facilitates the hydrolysis of pyrophosphate to orthophosphate [17].

Moreover, the ubiquity of phosphoryl transfer reactions in biochemistry poses the question of whether or not there is a general mechanism. The potential transition state structures range from totally dissociative, with an isolated metaphosphate intermediate, to totally associative, with a pentacoordinated phosphorus, depending on the electronic distibution. From an analysis of the changes in charge in the hydrolysis of GTP, derived from linear free energy relationships [18], it was concluded that the mechanism should be dissociative [19]. In the case of ATP, the oxygen that bridges the ß- with the γ–phosphates is expected to be the atom that develops the largest change of charge upon the transition state [20]. However, from the locations of the arginines obtained from the crystal structure of the UMP / CMP kinase from *Dictyostelium discoideum* [21], it was concluded that during the reaction negative charges are formed at the transferred phosphoryl group, but not at the phosphate bridging oxygen, and that this is consistent with an associative mechanism. More recent studies [22, 23] emphasize the importance of hydrogen bonding [22] and of the stabilization of the charges on the pyrophosphate oxygens [23] in the formation of the substrate-enzyme complexes, that suggest an associative mechanism with an "exploded"' transition state where the bond to the pyrophosphate leaving group is nearly broken and the bond with the incoming nucleophile is barely formed. Thus, qualitatively the mechanism is intermediate between associative and dissociative [20].

The theoretical attempts to elucidate the mechanism for the hydrolysis of pyrophosphates started with *ab initio* calculations of equilibrium structures [5, 24-26], and continued with the evaluation of electrostatic effects [7, 8], without taking into account metal dications. More recently, Ma *et al.* [27] performed *ab initio* calculations and found that the asymmetry of the electrostatic interactions induced by Mg^{2+} produced the elongation of one of the bridging P-O bonds with respect to the other. This allowed them to propose the isomerization [$Mg \cdot H_2P_2O_7$] → [$H_2PO_4 \cdot Mg \cdot PO_3$] as an intermediate step of the hydrolysis. Further studies were done to investigate the applicability of the same mechanism to anionic complexes [28, 29]. One of these studies [29] has shown that the Mg^{2+} cation can stabilize the dianionic complex [$HO \cdot Mg \cdot HP_2O_7$]$_2$.

Another study was made to explore the differences between complexation to calcium instead of magnesium [30], where the isomerization reaction enthalpies and energies resulted significantly higher for the calcium-pyrophosphates than for their magnesium counterparts, due mainly to a large positive contribution of correlation energy. It has recently been shown [31] that this effect is spurious because the lack of adequate *d* functions in the basis set used in Ref. [30] makes it incapable of effectively correlating the *3s* and *3p* electrons. Thus, the results that depend on correlation energies have to be revised. Moreover, though the geometries found in Ref. [30] were obtained from optimizations at the SCF level of theory, it is also worthwhile to revise the conclusion that the structural differences between the complexes of calcium and magnesium are dominated by the inherent coordination properties of their ions, and that they determine the differences in the energies of the isomerization reactions. These results suggest that the metallic ion involved plays quite an important role and, because of its intimate coordination with the pyrophosphate, this role must be prevalent in the catalytic site. Furthermore, it is known that the coordination properties of metallic ions are substantially different for each case and thus an analysis of the differences arising among a variety of pyrophosphate species coordinated to metallic cations can shed light on the mechanism of hydrolysis. Therefore, in this work we present a comparative study of anhydrous calcium- and zinc-pyrophosphates in their isomerizations to their metaphosphate containing counterparts:

$$[M \cdot H_N P_2O_7]^{(2-N)-} \rightarrow [H_N PO_4 \cdot M \cdot PO_3]^{(2-N)-} \qquad (1)$$

where N = 0, 1, 2, and M = Ca, Zn. Then, two approaches are made to study the effect of the aqueous environment on the relative stabilities of the structures that were found; first, an estimate of their solvation free energies by means of the polarizable continuum model of Cossi *et al.* (PCM [32]), and then by the interactions of the various complexes with a single water molecule,

$$H_2O + [M \cdot H_N P_2O_7]^{(2-N)-} \rightarrow [H_2O \cdot M \cdot H_N P_2O_7]^{(2\text{-}N)-}$$
$$H_2O + [H_N PO_4 \cdot M \cdot PO_3]^{(2-N)-} \rightarrow$$
$$[H_2O \cdot H_N PO_4 \cdot M \cdot PO_3]^{(2-N)-} \qquad (2)$$

Finally, the hydrolyses to M-orthophosphates were also considered:

$$H_2O + [M \cdot H_2P_2O_7] \rightarrow [H_2PO_4 \cdot M \cdot H_2PO_4]$$
$$H_2O + [M \cdot HP_2O_7]^- \rightarrow [H_2PO_4 \cdot M \cdot HPO_4]^-$$

$$H_2O + [M \cdot P_2O_7]^{2-} \rightarrow [HPO_4 \cdot M \cdot HPO_4]^{2-} \quad (3)$$

The recently designed 6-31+G* basis sets [33, 34] for Ca and Zn permit a refinement of the results previously found for Ca-phosphates [30], and a direct comparison with the Mg-phosphates, with the same accuracy. Thus, we can test the stability of the hydroxy anionic complexes $[HO \cdot Mg \cdot HP_2O_7]^{2-}$, and look into various possible routes for the hydrolysis of pyrophosphates that may explain the selectivity of the enzyme for Mg.

Computational Details

All electronic energies and harmonic vibrational frequencies were determined with the use of the GAUSSIAN98 [33] suite of programs. The standard basis set 6-31+G** was used for all atoms [34-36].

Geometry optimizations were performed with the SCF method. The order of these stationary-point structures was subsequently classified with calculated SCF harmonic frequencies from an analytically determined hessian. Unless otherwise stated, all reported equilibrium geometries correspond to structures in which the hessian eigenvalues are positive.

Single point energy calculations using Møller-Plesset second-order perturbation theory (MP2) were then performed on the SCF-optimized geometries to evaluate electron correlation contributions to the electronic energy.

The estimates of the energies ΔE_e^{SCF} and ΔE_e^{MP2} of the isomerizations and of the hydrolyses, as well as of the interactions with water, were computed with the SCF optimized geometries. The calculation of the enthalpies included a term ΔE_{th}^{298} that includes the zero-point energy (ZPE) and the thermal vibrational energy at T = 298.15 K, both computed with a harmonic approximation [37]:

$$\Delta H^o = \Delta E_e^{SCF} + \Delta E_e^{MP2} + \Delta E_{th}^{298} \quad (4)$$

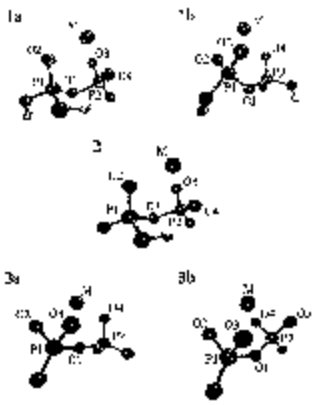

Fig. 1. Anhydrous $[M \cdot H_N P_2O_7]^{(2-N)-}$ complexes: structures **1a** and **1b** correspond to N = 2; structure 2 to N = 1, and structures **3a** and **3b** to N = 0. The staggered **3a** is optimal for M = Zn whereas the eclipsed **3b** is optimal for M = Ca; both are isoenergetic for M = Mg.

The reference state is at P = 0.1 MPa. The vibrational entropies were also computed with a harmonic approximation and a canonical partition function, and summed to the translational, the rotational and the electronic entropies according to standard statistical mechanics relationships [37]. The free energies were computed as the difference:

$$\Delta G = \Delta H - T\,\Delta S \quad (5)$$

To study the effect of the aqueous environment on the relative stabilities of the structures that were found, we made an estimate of their solvation free energies by means of the polarizable continuum model of Cossi *et al.* (PCM [32]).

An analysis of the charges on the dianionic complexes was made by means of Mulliken's population analysis [38] and of the CHELPG [39] scheme.

Results

In this section, the geometries of the Ca- and Zn-pyrophosphates, and the energies of their isomerizations and hydrolyses will be compared to their magnesium-containing counterparts. The data for these latter are taken from Ref. [29].

In the discussion of the structures depicted in Figs. 1-5, we will refer to the leftmost phosphorus with the three nonbridging oxygens bonded to it and the bridging oxygen as the orthophosphate moiety, and to the rightmost phosphorus with its respective three nonbridging oxygens as the metaphosphate moiety. Also, the abbreviation "M-PPi" will be used for the metal-pyrophosphate complexes.

Anhydrous isomerizations

M-pyrophosphates

The stationary geometries found for both $Zn \cdot H_2P_2O_7$ and $Ca \cdot H_2P_2O_7$ were the staggered configurations **1a** and **1b** (Fig. 1) that correspond to those previously found [29] for $Mg \cdot H_2P_2O_7$. In fact, the complexes with Zn have a very small deviation from their Mg-containing counterparts, whereas the complexes with Ca have Ca · O distances that are consistently longer than the Mg · O distances by ~ 0.4 Å (Table 1), in full agreement with the results of Ref. [30].

In the case of Ca, structure **1b** has a lower enthalpy (ΔH^o = –20.8 kJ / mol) and a lower free energy (ΔG^o = –25.4 kJ / mol) than **1a**, as it happened [29] with Mg. In the case of Zn the differences are small enough (ΔH^o = –1.2 kJ / mol and ΔG^o = 3.3 kJ / mol) to consider them isoenergetic. The asymmetry of the electrostatic interactions induced by the cation produces in both structures the elongation of one bridging P-O bond with respect to the other; the size of this effect being the same for the three cations, Mg, Ca and Zn: Δr = 0.2 Å for **1a**, and Δr = 0.07 Å for **1b** (Table 1).

The equilibrium geometries found for the monoanionic $[M \cdot HP_2O_7]^-$ complexes resulted very similar to their magnesium counterpart (structure **2** in Fig. 1). In all cases, the bridg-

Table 1. Geometrical parameters of M-pyrophosphatesa.

Structure	Mg	Ca	Zn	Mg	Ca	Zn	Mg	Ca	Zn
		P-O-P			r(M-O_1)			r(O_1-P_1)	
1a	120.6	121.2	121.5	2.998	3.368	2.968	1.544	1.542	1.544
1b	125.5	127.7	127.4	3.039	3.431	3.000	1.585	1.589	1.586
2	126.9	129.5	128.5	2.856	3.222	2.828	1.606	1.607	1.609
3a	139.3	154.9	138.5	2.665	2.468	2.678	1.611	1.649	1.612
3b	130.7	138.8	129.8	2.587	2.781	2.596	1.673	1.667	1.668
7a	119.5	120.9	120.2	3.038	3.383	3.037	1.544	1.541	1.545
7b	124.9	127.9	126.4	3.090	3.468	3.066	1.589	1.596	1.590
8	126.9	129.0	127.5	2.927	3.282	2.918	1.606	1.597	1.606
9a	138.6	153.7	139.3	2.744	2.453	2.744	1.597	1.631	1.601
9b	123.2	126.5	123.7	3.128	3.425	3.130	1.607	1.604	1.605
		r(O_1-P_2)			r(M-O_2)			r(M-O_3)	
1a	1.743	1.748	1.741	1.939	2.283	1.948	1.925	2.244	1.927
1b	1.660	1.650	1.655	2.009	2.328	2.028	2.013	2.336	2.041
2	1.663	1.663	1.661	1.878	2.203	1.876	1.924	2.236	1.932
3a	1.704	1.712	1.694	1.951	2.317	1.978	1.951	2.314	1.978
3b	1.673	1.667	1.668	2.053	2.340	2.058	2.053	2.340	2.058
7a	1.745	1.752	1.739	1.943	2.306	1.996	1.965	2.266	1.953
7b	1.657	1.640	1.651	2.032	2.343	2.077	2.035	2.365	2.060
8	1.663	1.671	1.660	1.930	2.268	1.946	1.935	2.253	1.936
9a	1.708	1.728	1.695	2.000	2.361	2.035	2.000	2.401	2.037
9b	1.668	1.674	1.670	1.985	2.315	1.992	2.029	2.398	2.171
		r(M-O_4)			r(M-O_3)				
1a	1.970	2.297	2.008						
1b	1.881	2.207	1.875						
2	1.963	2.276	2.011						
3a	1.840	2.183	1.834						
3b	2.053	2.341	2.058	2.053	2.341	2.058			
7a	2.017	2.322	2.034	2.031	2.461	2.032			
7b	1.911	2.261	1.907	2.024	2.407	2.026			
8	1.987	2.294	2.037	2.074	2.447	2.101			
9a	1.844	2.194	1.832	2.157	2.550	2.221			
9b	2.029	2.341	2.045	1.900	2.201	1.886			

[a] The P-O-P angle is in degrees and the distances in Å. The numbering of atoms corresponds to Figs. 1 and 3.

ing P-O bond of the proton free moiety is longer than the other, 1.66 Å *vs*. 1.61 Å, as a result of the asymmetry of the electrostatic interactions induced by the cation; the six non-bridging oxygens are in a staggered arrangement as viewed along an axis connecting the phosphorus atoms; the metal cation is coordinated to three oxygens. The > P-O-P < angle is very similar for the three cations, and once again the Ca · O distances are ~ 0.35 Å longer than for the other two cations (Table 1).

For the most relevant species in aqueous solution, the dianionic $[M \cdot P_2O_7]^{2-}$ complexes, two equilibrium geometries were determined with the SCF level of theory, one staggered and one eclipsed (**3a** and **3b**, respectively, Fig. 1). Though both configurations are very similar to their magnesium-containing counterparts, that are practically isoenergetic [28], in this case Ca^{2+} clearly favors the eclipsed configuration by ΔG^o = –43.3 kJ / mol, in agreement with Ref. [30]; whereas Zn^{2+} favors the staggered geometry by ΔG^o = –35.4 kJ / mol. In fact, the eclipsed configuration of $[Zn \cdot P_2O_7]^{2-}$ has one imaginary frequency and thus is not a minimum, but a transition state.

The different relative stabilities of structures **3a** and **3b** for the different cations are due to the balance among the attractive interactions of the cations with the oxygens in the pyrophosphate, the repulsive interactions of the oxygens and the strain induced on the structure of the pyrophosphate; thus, although the arrangement of oxygens in the vicinity of the cations roughly reproduces their respective coordination properties, there are some deviations due to the two excess electrons: the distances from the cations to the water molecules in their respective first hydration shells obtained from numerical simulations [40, 41] for Ca^{2+} range from 2.38 Å to 3.13 Å, for Mg^{2+} from 1.93 Å to 2.66 Å, and for Zn^{2+} from 1.82 Å to 2.74 Å. In the staggered configuration **3a**, each of the three cations is surrounded by three oxygens; the oxygen closest to the cation is at a significantly shorter distance for Ca (2.18 Å) and

Table 2. Geometrical parameters of M-metaphosphates and M-orthophosphates.[a]

Structure	Mg	Ca	Zn	Mg	Ca	Zn	Mg	Ca	Zn
		r(M-O_1)			r(M-O_2)			r(M-O_3)	
4	2.009	2.343	2.014	2.001	2.360	2.025	2.052	2.400	2.059
5	1.927	2.250	1.940	1.927	2.250	1.940	2.119	2.479	2.152
6a	2.039	2.329	2.053	2.039	2.329	2.053	2.039	2.329	2.069
6b	1.866	2.175	1.876	1.866	2.175	1.876	1.949	2.332	1.947
6c	1.873	2.181	1.884	1.873	2.181	1.884	2.218	2.584	2.278
10a	2.030	2.372	2.039	2.033	2.372	2.046	1.924	2.278	1.920
10b	2.080	2.379		2.080	2.375		2.130	2.481	
11	1.949	2.261	1.979	1.938	2.261	1.942	1.970	2.346	1.963
12a	2.112	2.398	2.087	2.035	2.331	2.028	2.112	2.398	2.087
12b	2.011	2.346	2.032	2.018	2.346	2.044	2.036	2.376	2.109
13	2.022	2.360	2.039	2.022	2.377	2.039	2.022	2.360	2.039
14	2.088	2.450	2.117	2.091	2.451	2.120	1.942	2.262	1.955
15	2.008	2.334	2.013	2.008	2.334	2.041	2.008	2.334	2.021
	r(M-O4)			r(M-O5)					
4	2.050	2.401	2.078						
5	2.119	2.479	2.152						
6a	1.963	2.346	1.961						
6c	2.218	2.584	2.283						
10a	2.020	2.390	2.048						
10b	2.074	2.418		2.057	2.424				
11	2.075	2.433	2.140						
12a	1.968	2.341	1.942	2.326	2.607	3.530			
12b	1.911	2.200	1.896						
13	2.022	2.377	2.039						
14	1.942	2.262	1.955						
15	2.008	2.334	2.022						

[a] Distances in Å. The numbering of atoms corresponds to Figs. 2, 4 and 5.

Table 3. Energies, enthalpies, entropies and solvation energies of the isomerizations of anhydrous M-pyrophosphates[a].

Reaction	ΔE_e^{SCF}	ΔE_e^{MP2}	ΔE_{th}^{298}	ΔH°	ΔS°	$\Delta\Delta G_{sol}$
M = Ca						
1a → **4**	–41.2	–3.7	–1.8	–46.7	65.3	127.1
1b → **4**	–7.3	–17.3	–1.3	–25.9	49.9	111.0
2 → **5**	–31.1	–6.5	–2.2	–39.8	64.8	148.1
3a → **3b**	–47.4	–2.3	0.5	–49.2	–19.8	16.3
3a → **6a**	–26.0	–7.2	–0.3	–33.5	87.6	126.5
3b → **6a**	21.4	–4.9	–0.8	15.7	107.4	110.2
3b → **6b**	66.3	–2.0	–0.6	63.7	89.7	52.9
3b → **6c**	65.3	–7.5	–0.6	57.2	65.1	69.4
M = Zn						
1a → **4**	–31.0	–9.6	–1.3	–41.9	52.6	104.3
1b → **4**	–16.3	–25.8	–1.0	–43.1	37.5	112.1
2 → **5**	6.3	–4.3	–1.9	0.1	59.5	94.7
3a → **3b**	39.5	–9.0	–2.8	27.7	–25.7	0.0
3a → **6a**	58.2	1.5	–0.9	58.8	73.4	137.7
3a → **6b**	29.9	–2.5	–0.3	27.1	67.6	86.9
3a → **6c**	62.6	–14.8	–3.1	44.7	25.3	87.3

[a] All energies and enthalpies in kJ / mol. Entropies are in J / (mol K). The last column has the differences in solvation free energies between reactants and products, computed with PCM [32].

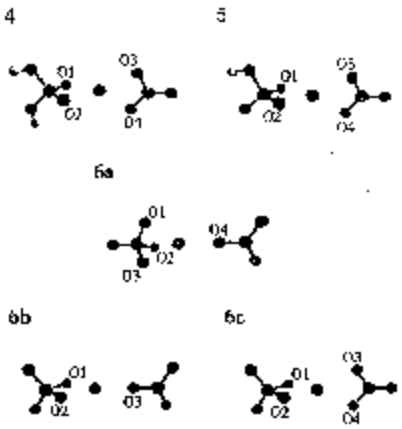

Fig. 2. Anhydrous putative $[H_NPO_4 \cdot M \cdot PO_3]^{(2-N)-}$ intermediates for the hydrolyses of M-PPi complexes. Structure 4 corresponds to N = 2; structure 5 to N = 1, and structures **6a**, **6b** and **6c** to N = 0. **6a** and **6b** are isoenergetic for M = Mg, whereas the global minimum for M = Ca is the former, and for M = Zn, the latter. Structure **6c** is isoenergetic to **6b** for M = Ca, and to **6a** for M = Zn.

for Mg (1.84 Å), whereas it remains at "hydration distance" from Zn (1.83 Å). In the eclipsed configuration **3b**, each of the three cations is surrounded by four oxygens at distances within their first hydration shells: 2.34 Å for Ca, 2.05 Å for Mg and 2.06 Å for Zn. In the case of Ca, also the bridging oxygen is at "hydration distance" in both configurations: 2.47 Å in 3a, and 2.78 Å in 3b, so the total coordination numbers grow to four and five, respectively. This can explain why the two structures are stable with Ca, and also their relative stabilities. The fact that the interaction of oxygen with Zn has a very deep minimum at short distance [41] favors the "tighter" coordination of **3a** over **3b**, because in the former it can overcome the oxygen-oxygen electrostatic repulsion, that the fourth oxygen makes so strong in **3b** as to make it a transition state. The coordination properties of Mg allow it to stabilize equally well both structures; though **3b** provides a more complete hydration, the oxygen-oxygen repulsion in **3a** is more easily overcome by the interactions with the cation.

As mentioned previously, the two excess electrons make the difference with respect to simple hydration: as it has been reported [29], the Mulliken analysis of the charges shows that there is a significant transfer of charge to the cation; in the eclipsed configuration the Mulliken charges on Mg and Zn are very similar, 0.49e and 0.42e, whereas for Ca it is 1.34e, and in the staggered configuration the values are 0.77e for Mg, 0.61e for Zn and 1.43e for Ca. Though not a definite test, these results suggest a more marked transfer of charge to Zn, a very similar effect for Mg, and a less important one for Ca. The energy gain due to this effect allows the staggered structure **3a** to be stable for both Ca and Mg, in spite of a coordination that is tighter than in simple hydration. An analysis of the effect of this transfer of charge on the bonds would be in order; unfortunately, because the positions of the ions in the $[M \cdot P_2O_7]^{2-}$ complexes make ring-like structures, the Hopf-Poincaré condition is not fulfilled [42] and thus the bond orders cannot be obtained. Nevertheless, the analysis of the Mulliken charges suggests that Mg and Zn withdraw a significant amount of electronic charge from their surrounding oxygens. A more complete discussion of the charge distribution will be made in section 3.4.

M-metaphosphate isomers

The anhydrous metaphosphates $H_2PO_4 \cdot M \cdot PO_3$ (**4**, Fig. 2) are also structurally similar to their magnesium counterpart: the two hydrogens remain attached to the moiety that becomes the orthophosphate coordinated to the cation by the two proton-free oxygens; the protons are hydrogen-bonded to the oxygens of the same moiety. The metaphosphate is also coordinated to the cation by two oxygens so that the metal has four total ligands in a tetrahedral configuration. As it was the case for the M-PPi complexes, the most notable differences among Mg-, Ca- and Zn-phosphates are the oxygen-metal bond distances, that for Zn are slightly longer than for Mg (between 0.05 Å and 0.10 Å) and shorter than for Ca (Table 2). This corresponds to the difference in the mean radii of their first hydration shells [40, 41]. Once again, the structural results of Ref. [30] are reproduced in the present work.

As it was mentioned in the introduction, the previously reported [30] free energy of the isomerization **1a** → **4** for Ca-pyrophosphate turned out to be largely positive (ΔG^o = 106.7 kJ / mol), due to spurious effects in the correlation energy. As expected [31], a well-balanced basis set produces a different value (Table 3); the free energy found in the present work (ΔG^o = –66.2 kJ / mol) was very similar to that of Mg-pyrophosphate (ΔG^o = –70.4 kJ / mol). The result for the iso-

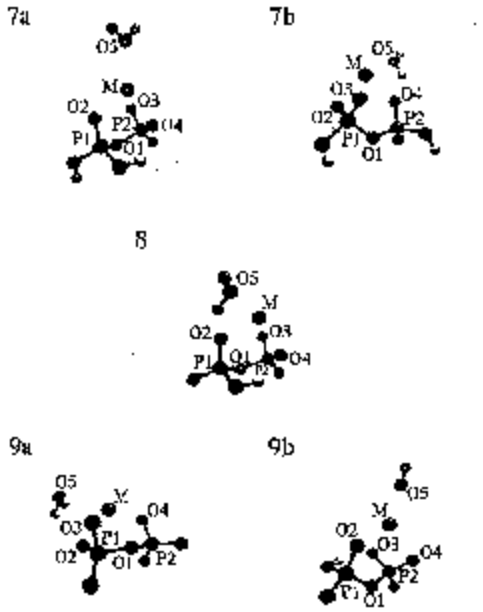

Fig. 3. Monohydrated $[H_2O \cdot M \cdot HNP_2O_7]^{(2-N)-}$ complexes. Structures **7a** and **7b** correspond to N = 2; the latter has a lower energy for the three cations. Structure **8** corresponds to N = 1, and structure **9a** to N = 0. The three ions stabilize the hydroxide anion found in **9b**, that has a much lower energy than **9a** (Tables 5 and 6).

merization of Zn-pyrophosphate was ΔG^o = –57.6 kJ / mol (Table 6). The contribution of solvation energies obtained with the PCM model made a large difference: the free energy became largely positive for both Ca- and Zn-pyrophosphates, whereas it remained negative for Mg-pyrophosphate (Tables 3 and 6).

The isomerization **1b** → **4** yields very similar results to **1a** → **4**, though the estimated effect of the solvent is larger in the case of Zn-PPi, and smaller in the case of Ca-PPi (Tables 3 and 6).

The isomerization product $[HPO_4 \cdot M \cdot PO_3]^-$ is structure **5** (Fig. 2). The behavior of the cation-oxygen distances is the same as that found for the hydration shells of the metal cations [40, 41] (Table 2). The calculated free energy of the isomerization **2** → **5** is largest for the calcium complexes, ΔG^o = –59.1 kJ / mol, and smallest for the zinc complexes, ΔG^o = –17.7 kJ / mol (Tables 3 and 6).

Three stationary geometries were found for the dianionic metaphosphate isomer $[PO_4 \cdot M \cdot PO_3]^{2-}$; we have found it convenient [29] to label them by the number of oxygens from the orthophosphate and from the metaphosphate coordinated to the cation, so the structures are a 3 × 1 (**6a**, Fig. 2), a 2 × 1 (**6b**, Fig. 2), and a 2 × 2 (**6c**, Fig. 2) configurations. Though **6a** and **6c** have four oxygens coordinated to the cation, the Zn · O distances are longer. This results in considerably higher energies compared to the optimal geometry **6b**, ΔG^o = 30 kJ / mol. Once again, Zn^{2+} coordination depends more on bringing the ligands closer than increasing their number in the first shell.

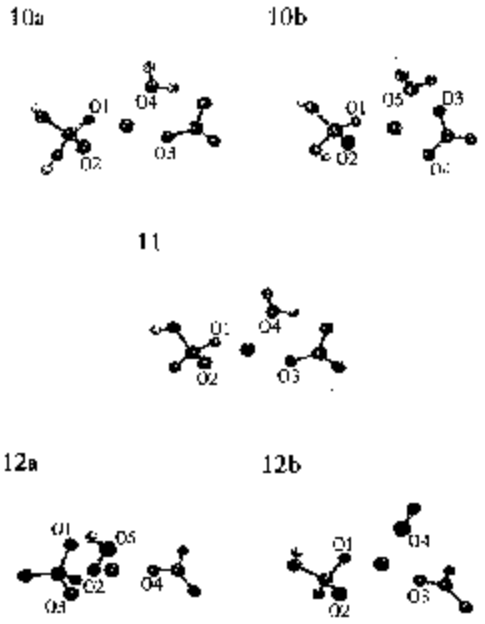

Fig. 4. Monohydrated putative $[H_2O \cdot H_NPO_4 \cdot M \cdot PO_3]^{(2-N)-}$ intermediates for the hydrolyses of the M-PPi complexes. Structures **10a** and **10b** correspond to N = 2; the latter was not found for M = Zn. Structure **11** corresponds to N = 1, and structure **12a** to N = 0. Once again, the three ions stabilize the hydroxide anion in **12b**, with a much lower energy than **12a**, but still higher than **9b** (Tables 5 and 6).

The Mulliken charges on Zn show the same oxidizing power as for the pyrophosphates: 0.99e in 6a, 0.63e in 6b and 0.66e in 6c. In the case of Ca^{2+}, the 2 × 1 configuration has an energy similar to the 2 × 2, both being higher than the 3 × 1 by ΔG^o = 40 kJ / mol, and the Mulliken charges are 1.43*e* in **6a**, 1.51*e* in **6b** and 1.54*e* in **6c**. For Mg^{2+}, the 3 × 1 geometry is virtually isoenergetic to 2 × 1, ΔG^o = 6.4 kJ / mol, and the Mulliken charges are 1.00*e* in the former and 0.83*e* in the latter. The situation of the metaphosphate isomers is similar to that for the pyrophosphate complexes: due to their distinctly different coordination properties, and to their different oxidizing powers, the three cations favor different geometries; thus Ca^{2+} favors more ligands in the first shell, Mg^{2+} makes the two configurations isoenergetic, and Zn^{2+} favors the geometry that has the oxygens of the first shell closer to the cation. This repeated pattern can be seen in Tables 1 and 2, where a comparison is made of the M · O distances between the various equilibrium geometries found for all the M-pyrophosphates and the M-phosphates, where M = Ca, Mg, Zn.

The isomerization **3a** → **6b** is predicted to be endothermic for Zn^{2+}, ΔH^o = 27 kJ / mol; the change in entropy accounts for a smaller, but still positive free energy, ΔG^o = 7 kJ / mol (Tables 3 and 6). In the case of Ca^{2+}, the isomerization **3b** → **6a** is also predicted to be endothermic, ΔH^o = 16 kJ/mol, but the change in entropy is large enough to yield a negative free energy, ΔG^o = –16 kJ / mol. However, the contribution of solvation leads to the same result as for Zn^{2+}, a largely positive free energy, ΔG_{aq} = 94 kJ / mol, whereas in the case of Mg^{2+} it is this contribution that leads to a negative free energy of the isomerization **3b** → **6b** [29].

Isomerizations of monohydrated species

The approximation with a continuum model to account for hydration effects is obviously too restrictive when looking into a process where one water molecule gets broken. Therefore in this section the study is extended to explicitly include that water molecule.

M-pyrophosphates

The equilibria of structures **1a** and **1b** with one water molecule produced the stationary configurations **7a** and **7b**, respectively (Fig. 3). For both cations, the perturbation on the geometries of the M-pyrophosphates turned out to be rather small; the difference produced on the bond lengths was of less than 0.05 Å, and on the bond angles of less than 1º (Table 1). In structure **7a**, the hydrogens of the water molecule point to a direction away from the pyrophosphate, whereas in **7b** one of them makes a hydrogen-bond with an oxygen of the metaphosphate moiety. This feature is more pronounced for the monoanionic structure **8** (Fig. 2), that results from the interaction of water with structure **2**, and even more for the dianionic species **9a**, but in this case the hydrogen-bond is made with the orthophosphate moiety. In all cases, the interaction with the water molecule is characterized by a largely negative enthalpy and by a largely negative change in entropy,

Table 4. Enthalpies, entropies and free energies of the interactions of M-phosphates with one water molecule[a].

Reaction	$\Delta H°$	$\Delta S°$	$\Delta G°$	$\Delta\Delta G_{sol}$	ΔG_{aq}
M = Ca					
1a + H_2O → **7a**	–107.3	–126.6	–69.6	57.4	–12.2
1b + H_2O → 7b	–117.8	–135.1	–77.5	80.8	3.3
2 + H_2O → **8**	–114.7	–123.7	–77.8	41.3	–36.5
2 + OH^- → **9b**[b]	–199.6	–119.5	–164.0	153.3	–10.8
3a + H_2O → **9a**	–135.5	–140.0	–93.7	100.2	6.5
3b + H_2O → **9b**[c]	–330.0	–130.3	–291.2	266.4	–24.8
4 + H_2O → **10a**	–82.2	–131.5	–43.0	23.5	–19.5
4 + H_2O → **10b**	–90.5	–116.5	–55.8	47.4	–8.4
5 + H_2O → **11**	–72.2	–125.0	–34.9	16.5	–18.4
5 + OH^- → **12b**[b]	–66.9	–91.3	–39.7	20.6	–19.1
6a + H_2O → **12a**	–130.2	–176.3	–77.6	136.9	59.3
6b + H_2O → **12b**[c]	–252.7	–144.8	–209.5	171.7	–37.8
M = Zn					
1a + H_2O → **7a**	–119.0	–78.3	–95.7	105.8	10.1
1b + H_2O → **7b**	–137.4	–110.8	–104.4	66.0	–38.4
2 + H_2O → **8**	–97.3	–131.6	–58.1	42.9	–15.2
2 + OH– → **9b**[b]	–181.6	–123.7	–144.7	67.0	–77.7
3a + H_2O → **9a**	–100.6	–136.2	–60.0	100.1	40.1
3b + H_2O → **9b**[c]	–327.3	–125.7	–289.8	215.0	–74.8
4 + H_2O → **10a**	–82.8	–132.8	–43.3	7.5	–35.8
5 + H_2O → **11**	–72.3	–135.9	–31.8	8.3	–23.5
5 + OH^- → **12b**[b]	–62.0	–105.2	–30.6	–49.1	–79.7
6b + H_2O → **12a**	–63.6	–159.0	–16.2	100.7	84.5
6b + H_2O → **12b**[c]	–207.0	–141.0	–165.0	90.5	–74.5

[a] All energies and enthalpies are in kJ / mol. Entropies are in J / (mol K).

[b] Interactions of monoanionic M–phosphates with a hydroxide anion.

[c] In these cases the water molecule releases a proton to the phosphate and the resulting hydroxide remains coordinated by the metal cation. The last two columns are the differences in solvation free energies between reactants and products, and the free energies in aqueous solution, computed with PCM [32]. The latter was computed as $\Delta G_{aq} = \Delta G° + \Delta\Delta G_{sol}$.

the latter coming from the restrictions on the motion of the water molecule; however, all the free energies still turned out to be largely negative (Table 4).

The optimal configuration of the monohydrated dianionic M-pyrophosphates is structure **9b**, where the water molecule was hydrolyzed into a proton that binds to one of the oxygens of the pyrophosphate, and a hydroxide anion, that gets coordinated by the metal cation. The free energies of the reactions $H_2O + [M \cdot P_2O_7]^{2-} \rightarrow [HO \cdot M \cdot HP_2O_7]^{2-}$, were even larger than for the simple interactions of the previous paragraph (Table 4). The resulting M-pyrophosphates have an intramolecular hydrogen-bond that contributes to the bending of the > P-O-P < angle by more than 12º, relative to their anhydrous counterparts (Table 1). Both **9a** and **9b** are staggered configurations, showing that in the eclipsed geometry the pyrophosphate is subject to a strain, that is released when one of its oxygens coordinated by the cation can be substituted.

Structure **9b** can also be viewed as the monoanionic M-pyrophosphate **2** interacting with a hydroxide anion [29]. The interaction energies computed from **2** + OH^- → **9b** for M = Ca and Mg are very similar, $\Delta G°$ = –164 kJ / mol *vs.* $\Delta G°$ = –162 kJ / mol, whereas for Zn it is somewhat smaller, $\Delta G°$ = –145 kJ / mol (Table 4).

Hence the inclusion of a water molecule makes no appreciable difference for the neutral and monoanionic species, whereas for the dianionic cases it readily leads to the water hydrolysis.

M-metaphosphate isomers

The interaction energies of the neutral M-metaphosphate complexes with one water molecule, **4** + H_2O → **10a** (Fig. 4), were large and very similar for the three cations, $\Delta G° \approx$ –44.0 kJ / mol. However, the structure 10b, that turned out to be more stable for M = Mg and M = Ca, was not found for M = Zn. It is worth noticing that in 10a the cation coordinates four oxygens, whereas in 10b it coordinates five oxygens.

In agreement with previous results [29], the interaction with one water molecule stabilized the M-pyrophosphates with respect to the M-metaphosphates (Tables 4, 5 and 6). This effect was enhanced by the solvation free energies. Thus, the isomerizations from structures **7a** and **7b** to structures **10a** and **10b** were all predicted as non-spontaneous in aqueous solution, with the exception of **7a** → **10a** in the case of zinc, whose free energy turned out to be ΔG_{aq} = 0.8 kJ / mol.

The interaction of the monoanionic M-metaphosphate complexes with one water molecule leads to structure **11** (Fig.

Table 5. Energies, enthalpies, entropies and solvation energies of the isomerizations of monohydrated M-pyrophosphates[a].

Reaction	ΔE_e^{SCF}	ΔE_e^{MP2}	E_{th}^{298}	$\Delta H°$	$\Delta S°$	$\Delta\Delta G_{sol}$
M = Ca						
7a → **10a**	–21.9	–1.5	1.7	–21.7	60.4	93.2
7b → **10a**	22.3	–11.2	–1.5	9.6	53.5	53.7
7a → **10b**	–24.9	–6.0	1.1	–29.8	75.4	117.1
7b → **10b**	19.3	–15.8	–2.1	1.4	68.5	77.6
8 → **11**	2.8	1.6	–1.6	2.8	63.5	94.3
9a → **9b**	–272.8	31.2	–2.1	–243.7	–10.0	146.4
9a → **12a**	–23.0	–5.5	0.2	–28.3	51.4	127.1
9b → **12b**	96.6	–0.6	–2.9	93.1	92.9	15.5
M = Zn						
7a → **10a**	–3.3	–2.7	0.3	–5.7	–1.8	6.0
7b → **10a**	25.0	–13.6	0.0	11.6	15.5	53.6
8 → **11**	18.4	8.2	–1.6	25.0	55.3	60.1
9a → **9b**	–229.0	32.5	–2.5	–199.0	–15.2	114.9
9a → **12a**	62.9	5.4	–4.2	64.1	44.9	87.5
9b → **12b**	122.0	0.0	–2.3	119.7	78.0	–21.4

[a] All energies and enthalpies are in kJ / mol. Entropies are in J / (mol K). The last column has the differences in solvation free energies between reactants and products, computed with PCM [32].

Table 6. Comparison of the isomerizations free energies of M-pyrophosphates[a].

Reaction	$\Delta G°$			ΔG_{aq}		
	Mg	Ca	Zn	Mg	Ca	Zn
1a → **4**	–70.4	–66.2	–57.6	–18.1	60.9	46.7
1b → **4**	–64.1	–40.8	–54.3	2.5	70.2	57.8
2 → **5**	–39.6	–59.1	–17.7	–8.1	89.0	77.0
3a → **6b**	1.1	–6.4	6.9	12.4	62.8	93.8
3b → **6a**	8.8	–16.3	1.5	23.2	93.9	139.2
7a → **10a**	–10.0	–39.7	–5.2	36.4	53.5	0.8
7a → **10b**	–17.1	–52.3		22.7	64.8	
7b → **10a**	3.9	–6.4	6.8	44.9	47.3	60.4
7b → **10b**	–3.1	–19.0		31.3	58.6	
8 → **11**	–4.9	–16.1	8.5	22.5	78.2	68.6
9a → **9b**	–213.3	–240.7	–194.5	–117.5	–94.3	–79.6
9a → **12a**	12.6	–43.6	50.7	82.0	83.5	138.2
9b → **12b**	82.9	65.4	96.4	83.6	81.0	75.0

[a] All energies are in kJ / mol. The free energy in aqueous solution was computed as $\Delta G_{aq} = \Delta G° + \Delta\Delta G_{sol}$.

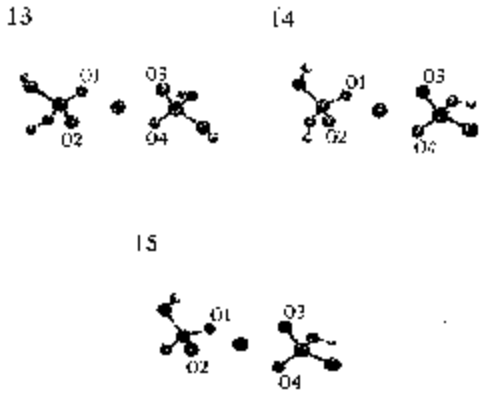

Fig. 5. Hydrolyzed M-orthophosphates. Structure **13** corresponds to the neutral $[H_2PO_4 \cdot M \cdot H_2PO_4]$ complex; structure **14** to the $[H_2PO_4 \cdot M \cdot HPO_4]^-$ complex, and structure **15** to the $[HPO_4 \cdot M \cdot HPO_4]^{2-}$ complex. This latter turned out to be isoenergetic to **9b**, but when solvation is taken into account the hydrolyses **9b** → **15** are predicted to be spontaneous (Table 8).

4), and in all cases it is weaker than the interaction of the M-pyrophosphates. The interaction with water stabilizes the M-pyrophosphates to such an extent that the isomerization **8** → **11** becomes endothermic and non-spontaneous for M = Zn (Tables 4, 5 and 6). The estimates of the solvation free energies produce the same result, the stabilization of M-pyrophosphates.

As it occurred with the anionic M-pyrophosphates, the interaction of structures **6a** and **6b** with a water molecule led to a stationary state with a water molecule, **12a**, and a very stable configuration with a hydroxide anion, **12b** (Fig. 4), even considering the free energies of solvation. The isomerization **9b** → **12b** turned out to be endothermic and non-spontaneous in all cases, whereas the isomerization **9a** → **12a** turned out to be exothermic and spontaneous for M = Ca. However, the free energy of solvation shifted towards non-spontaneity in all cases (Tables 4, 5 and 6).

It is worth noticing the relatively large contribution of the entropy to the estimates of the isomerization free energies. The data presented in Tables 3, 4 and 5 were obtained from standard statistical mechanics [37] applied to the harmonic frequencies computed from second derivatives of the energies. Typically, a scaling factor of 0.9 is applied to the theoretical SCF frequencies [37]. This scaling would affect the thermal energy ΔE_{th}^{298} and the vibrational contribution to the entropy, that are a small percentage of the total enthalpy and entropy;

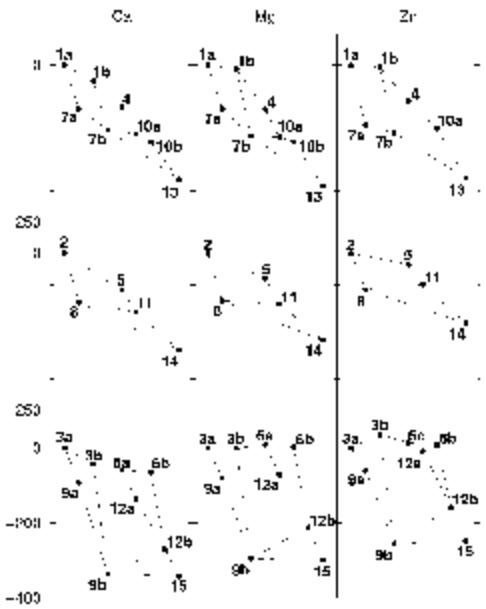

Fig. 6. Schematic comparison of the relative free energies ΔG^o (in kJ / mol, vertical axis) for the stationary states found in this work, referred to structures **1a**, **2** and **3a** in each case. From top to bottom, the neutral, monoanionic and dianionic complexes. From left to right, M = Ca, M = Mg and M = Zn. The lines drawn as a reference correspond to the reactions in Tables 4, 6 and 8.

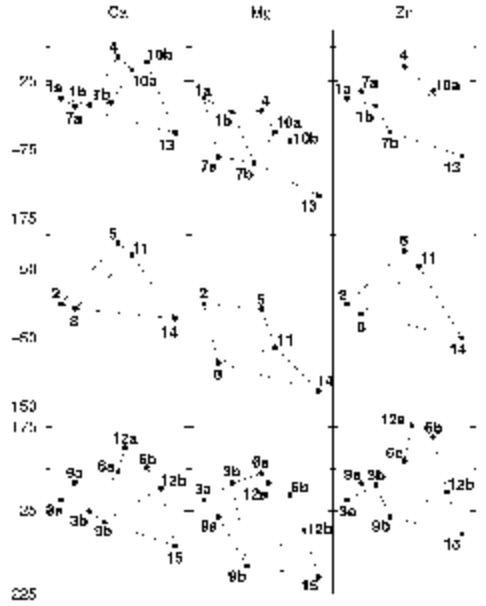

Fig. 7. Schematic comparison of the relative free energies in aqueous solution ΔG_{aq} (in kJ / mol, vertical axis) for the stationary states found in this work, referred to structures **1a**, **2** and **3a** in each case. They were computed as $\Delta G_{aq} = \Delta G^o + \Delta\Delta G_{sol}$, the latter term obtained with PCM [32]. From top to bottom, the neutral, monoanionic and dianionic complexes. From left to right, M = Ca, M = Mg and M = Zn. The lines drawn as a reference correspond to the reactions in Tables 4, 6 and 8.

nevertheless, to assess a quantitative estimate of the accuracy of our calculations, we computed the vibrational contributions with scaling factors of 0.9 and 1.1 on the frequencies. The total effect on the free energies is less than ±5 kJ / mol in all cases. Therefore, the qualitative conclusions for the isomerizations are not modified, exception made of the reaction **9a** → **12b** for Zn^{2+}, that has a value in the limits of accuracy of this study, ΔG_{aq} = –4.6 kJ / mol, and thus could be reversible. At any rate, this is still in agreement with the experimental observation that Zn-pyrophosphate can be used as substrate by pyrophosphatases.

Hydrolysis reactions

The optimal geometry found for the product $H_2PO_4 \cdot M \cdot H_2PO_4$ (structure **13**, Fig. 5) has the metal cation aligned with the phosphorus atoms and coordinating four oxygens, two from each phosphate, forming two O-M-O orthogonal planes, quite similar to structure **4**. The Zn · O distances are only 0.02 Å longer than the Mg · O, whereas the Ca · O distances are 0.34 Å longer. The hydrolysis **7a** → **13** was predicted to be both exothermic and spontaneous (Tables 7 and 8), with very similar free energies for Mg and Zn complexes. The effect of solvation in Zn-PPi is opposite to Mg-PPi and Ca-PPi, for it enhances the hydrolysis. The reaction **7b** → **13** was also predicted to be both exothermic and spontaneous (Tables 7 and 8), with very similar free energies for the three cations. The effect of solvation is most marked for Zn-pyrophosphate, so the predicted free energy in aqueous solution is 72 % of the value for Mg-pyrophosphate.

The optimized geometry of the $[H_2PO_4 \cdot M \cdot HPO_4]^-$ complexes is structure **14** (Fig. 4) and has the same features as structure **13**. The hydrolysis **8** → **14** reproduces the trend of the isomerization **2** → **5**, with a largest free energy for calcium and a smallest for Zn, and a most marked effect of hydration on the calcium complexes (Tables 6, 7 and 8).

The fully hydrolyzed dianionic complex resulted in structure **15**, where the cation coordinates four oxygens, in a 2 × 2 arrangement. The predicted free energies of the hydrolyses **9b** → **15** are rather small (Tables 7 and 8), in the limits of accuracy of the *ab initio* method employed. Opposite to the isomerizations to a metaphosphate intermediate, the contribution of solvation leads to negative free energies in all cases.

Analysis of the charge distribution on the dianionic M-PPi and M-Pi complexes

Because all schemes to assign atomic charges are somewhat arbitrary, we decided to use two different approaches: (1) one that yields information of the electron density in the vicinity of each atom, Mulliken's population analysis [38], and (2) one that yields information of the electrostatic potential, the CHELPG scheme [39]. This latter was preferred over the previously used [29] CHELP [43] because it is less sensitive to changes in the orientations of the molecules [39]. The values obtained from CHELPG still depend on the van der Waals

Table 7. Energies, enthalpies, entropies and solvation energies of the hydrolyses of M-pyrophosphates[a].

Reaction	ΔE_e^{SCF}	ΔE_e^{MP2}	ΔE_{th}^{298}	ΔH°	ΔS°	$\Delta\Delta G_{sol}$
M = Ca						
7a → **13**	–137.5	34.3	1.6	–101.6	37.6	74.3
7b → **13**	–93.3	24.5	–1.6	–70.4	30.7	34.8
8 → **14**	–98.9	36.4	–2.0	–64.5	39.3	62.3
9b → **15**	–18.9	19.8	1.9	2.8	35.7	–49.5
M = Zn						
7a → **13**	–120.1	28.5	–0.3	–91.9	–23.7	–9.7
7b → **13**	–91.8	17.6	–0.6	–74.8	–6.3	37.9
8 → **14**	–76.4	36.4	–2.8	–42.8	35.8	18.9
9b → **15**	–2.9	17.1	0.9	15.1	27.8	–47.9

[a] All energies and enthalpies are in kJ / mol. Entropies are in J / (mol K). The last column has the differences in solvation free energies between reactants and products, computed with PCM [32].

Table 8. Comparison of the hydrolysis free energies of M-pyrophosphates[a].

Reaction	?G°			?Gaq		
	Mg	Ca	Zn	Mg	Ca	Zn
7a → **13**	–87.1	–112.8	–84.8	–61.0	–38.5	–94.5
7b → **13**	–73.2	–79.6	–72.9	–48.5	–44.8	–35.0
8 → **14**	–62.7	–76.3	–53.5	–40.1	–14.0	–34.6
9b → **15**	–4.4	–7.9	6.8	–26.4	–57.4	–41.1

[a] All energies are in kJ / mol. The free energy in aqueous solution was computed as $\Delta G_{aq} = \Delta G° + \Delta\Delta G_{sol}$.

radii given to the various atoms; in this case they were: 2.00 Å for P, 1.70 Å for O and 1.45 Å for H, as standard *Breneman* radii in GAUSSIAN98; whereas for the metal cations they were taken from Ref. [44]: 1.73 Å for Mg, 2.00 Å for Ca, and 1.39 Å for Zn.

The results are shown in Table 9, where it can be seen that the cations withdraw a substantial amount of negative charge, with the oxydizing power in the order Zn ≥ Mg > Ca. In all cases, the Mulliken charge on the bridging oxygen in both **3a** and **3b** is large and negative, showing a high electron density around it; the CHELPG charge is smaller, but still significant, and reflects an anionic electrostatic potential. The Mulliken charges on the phosphoryl moieties show a lower electron density, but the CHELPG charges reflect a higher electrostatic potential, thus making the phosphoryl moieties susceptible of strong electrostatic interactions, but with a low probability of chemical bonding. Upon isomerization to **6a**, **6b** and **6c**, the Mulliken negative charge on the bridging oxygen diminishes while the CHELPG charge increases; thus the electron density is lower, but the anionic field stronger. The behavior of the monohydrated complexes **9a** and **12a** shows the same trend, that remains equal for the complexes with hydroxide anions **9b** and **12b**.

Discussion and conclusions

The results presented in the preceeding section show the structural differences imposed by the cations on pyrophosphate, due to their distinctly different coordination properties, that in the case of Ca^{2+} favor a larger amount of ligands in its first hydration shell, whereas in the case of Zn^{2+} favor "tighter" structures, where the ligands are at shorter distances from the cation. The properties of Mg^{2+} allow for both types of coordination, so the Mg-pyrophosphate and Mg-phosphate complexes can adopt the conformations of both zinc-complexes and calcium-complexes.

Although the hydrolysis of pyrophosphates in living cells occurs in a specific environment, determined by the catalytic site of the enzyme [14, 45, 46], theoretical studies of the reactions *in vacuo* are helpful to discriminate intramolecular effects from the contributions of various intermolecular interactions. In this case, based on a previous study [30], the differences in coordination properties between ions were proposed as an explanation for the experimental data that the membrane-bound pyrophosphatase of *Rhodospirillum rubrum* can utilize zinc complexes as substrates for the hydrolysis of pyrophosphates, with a slightly smaller efficiency, and a distinct concentration dependent kinetics, than those for magnesium containing complexes, whereas they cannot utilize calcium complexes [9, 15]. The results obtained in the present work support that proposal.

The structural differences found to occur in the equilibrium geometries of the Zn-pyrophosphate complexes and their isomerization products, relative to their magnesium-containing counterparts, are mainly due to a more rigid coordination by Zn^{2+}. The 2 × 1 geometry found for the dianioninc complex $[PO_4 \cdot Zn \cdot PO_3]^{2-}$ allowed for a more complete study of the isomerization products of Ca-pyrophosphates and Mg-pyrophosphates; the coordination properties of Ca^{2+} favor the 3 × 1 configuration, that has more ligands in the first shell; Mg^{2+} makes the 2 × 1 and the 3 × 1 configurations virtually isoenergetic, and Zn^{2+} favors the 2 × 1 geometry, that has the ligands closer to it than in the 3 × 1 geometry.

The interactions of the complexes with one water molecule are all characterized by a large enthalpy and a large decrease in entropy (Table 4). This reflects mainly the strong interaction with the metal cation as well as the restriction imposed by its coordination properties on the positions attainable by the water molecule. ΔH – TΔS compensatory relationships have also been found in a study of the thermodynamics of phosphate and pyrophosphate anions binding by polyammonium receptors [22], where hydrogen bonding is found to be crucial in anion coordination. In agreement with a previous result [29], the interactions of the dianionic M-pyrophosphate complexes lead readily to the breaking of the water molecule, producing very stable $[HO \cdot M \cdot HP_2O_7]^{2-}$, complexes. This supports the previously advanced idea that a hydroxide anion can be stabilized by the metallic cation in the catalytic site.

Table 9. Charges on dianionic M-Phosphates[a].

Structure	M	O	PO_3	PO_3	Structure	M	O	PO_3	PO_3	H_2O
3a					**9a**					
Mg	0.77	–1.48	–0.53	–0.76		0.66	–1.47	–0.62	–0.74	0.17
	1.51	–0.84	–1.32	–1.35		1.50	–0.81	–1.35	–1.33	–0.01
Ca	1.43	–1.64	–0.89	–0.90		1.44	–1.62	–0.99	–0.86	0.03
	1.63	–0.87	–1.39	–1.37		1.64	–0.86	–1.38	–1.36	–0.04
Zn	0.61	–1.48	–0.48	–0.65		0.58	–1.47	–0.61	–0.66	0.16
	1.33	–0.85	–1.24	–1.24		1.35	–0.81	–1.27	–1.26	–0.01
3b					**9b**			HPO_3		HO
Mg	0.49	–1.35	–0.57	–0.57		0.88	–1.47	–0.06	–0.66	–0.70
	1.47	–0.75	–1.36	–1.36		1.48	–0.79	–0.54	–1.32	–0.83
Ca	1.34	–1.40	–0.97	–0.97		1.54	–1.43	–0.22	–1.02	–0.87
	1.61	–0.77	–1.42	–1.42		1.76	–0.82	–0.60	–1.39	–0.95
Zn	0.42	–1.50	–0.46	–0.46		0.81	–1.46	–0.02	–0.66	–0.67
	1.34	–0.78	–1.28	–1.28		1.40	–0.81	–0.52	–1.29	–0.78
6a					**12a**			PO_3		H_2O
Mg	1.00	–1.28	–0.91	–0.81		0.88	–1.25	–0.92	–0.80	0.09
	1.43	–1.19	–1.38	–0.86		1.46	–1.16	–1.39	–0.88	–0.03
Ca	1.43	–1.32	–1.17	–0.94		1.43	–1.30	–1.21	–0.94	0.02
	1.63	–1.25	–1.45	–0.93		1.65	–1.21	–1.46	–0.94	–0.04
Zn	0.99	–1.28	–0.88	–0.83		0.99	–1.27	–0.93	–0.80	0.01
	1.36	–1.17	–1.31	–0.88		1.34	–1.12	–1.32	–0.87	–0.03
6b					**12b**			HPO_3		HO
Mg	0.83	–1.16	–0.90	–0.77		0.86	–1.12	–0.19	–0.83	–0.72
	1.30	–1.16	–1.33	–0.81		1.51	–1.11	–0.63	–0.93	–0.84
Ca	1.51	–1.35	–1.22	–0.94		1.59	–1.27	–0.49	–0.95	–0.88
	1.62	–1.27	–1.42	–0.93		1.75	–1.13	–0.72	–0.96	–0.94
Zn	0.63	–1.08	–0.88	–0.67		0.81	–1.10	–0.21	–0.83	–0.67
	1.31	–1.16	–1.29	–0.86		1.43	–1.10	–0.59	–0.94	–0.80
6c					**15**		HPO_3	HPO_3		
Mg						0.68	–1.33	–1.35		
						1.43	–1.71	–1.72		
Ca	1.54	–1.35	–1.22	–0.97		1.53	–1.77	–1.76		
	1.61	–1.28	–1.42	–0.91		1.67	–1.84	–1.83		
Zn	0.66	–1.07	–0.91	–0.68		0.64	–1.31	–1.33		
	1.30	–1.16	–1.29	–0.85		1.38	–1.69	–1.69		

[a] Charges in e. For each element, the first row shows the charges obtained from Mulliken's population analysis [38], and the second row, those obtained from the CHELPG scheme [39].

Moreover, the hydroxide anion is stable even taking into account the solvation energies (Table 4) so the theoretical prediction is that the dissociation of a water molecule should occur in the aqueous solution. This seems contradictory to experimental data [47] of aqueous solutions of $HP_2O_7^{3-}$ at pH 7.0; when either Mg or Zn is added, the change in pH shows that a proton is released from the complex, that should thus be converted into $[M \cdot HP_2O_7]^{2-}$. The theoretical prediction obtained here and in a previous work [29] leads to conclude that the proton is released from one water molecule, leaving a hydroxide anion attached to the complex. The permanence of such a complex depends on the exchange rate between the first and the second hydration shells. The results from nuclear magnetic resonance experiments [48] show that this rate is slow for both Mg^{2+} and Zn^{2+}, whereas it is somewhat faster for Ca^{2+}. It has been shown in numerical simulations [40, 41] that this is due to the fact that both Mg^{2+} and Zn^{2+} have a depletion layer between their respective first and second hyration shells, where neither oxygens nor hydrogens are present, this being strict for Mg^{2+} and a little less so for Zn^{2+}. On the other hand, Ca^{2+} allows hydrogens in the region between its first and second hydration shells, a situation that would immediately conduce to the transfer of the hydroxide anion to the bulk, by means of proton exchanges (*proton jumps*). Thus, the

former two cations should be able to maintain the hydroxide anion attached more easily than the latter. This would make a rather important difference because Mg-PPi and Zn-PPi would carry their nucleophile into the active site of the enzyme, whereas Ca-PPi would not be able to do the same.

The relative gas-phase free energies of the various stable configurations found in this work are depicted in the graphs of Fig. 6. The effect of solvation can be seen in the corresponding graphs of Fig. 7. For the completely anhydrous complexes, the energies of the isomerizations of the Zn-pyrophosphates are somewhat higher than those of the Mg-pyrophosphates, whereas for the Ca-pyrophosphates these energies are consistently lower (Table 8). Thus, it would seem that the hydrolysis through a metaphosphate intermediate should be facilitated by calcium; however, when the solvation energy is taken into account, the picture changes: Ca-pyrophosphates become generally more stable with respect to their metaphosphate isomers than Mg- and Zn-pyrophosphates. These results allow for a reconsideration of the previously proposed dissociative mechanism [29]: the species entering the catalytic site should have structure **9b**. The hydroxide anion would be attracted by the metallic cation in the catalytic site, and substituted by a water molecule, thus converting the dianionic **9b** into the monoanionic **8**. This latter can be anchored in the catalytic site [14] and isomerize to **11**. The results in Table 8 show that this reaction should be spontaneous for anhydrous Ca-PPi and Mg-PPi, and reversible for Zn-PPi; though the effect of full solvation is to impede these isomerizations in the three cases (compare Fig. 6 to Fig. 7), it is to be expected [14, 45, 46] that the catalytic site regulates the amount of water molecules that surround the substrate, thus permitting the variation of the free energies of the isomerizations. It is to be noted that this mechanism requires the M-PPi complex to carry its own nucleophile inside the catalytic site; this is possible for fully hydrated Mg-PPi and Zn-PPi, whereas Ca-PPi would lose the hydroxide anion in the aqueous solution. This would explain why the hydrolyses of both Mg- and Zn-pyrophosphates can be catalyzed by the enzyme, whereas the hydrolysis of Ca-pyrophosphate cannot.

Recent studies [49, 50] on phosphate ester hydrolysis in aqueous solutions compared the associative *vs.* the dissociative mechanisms, and showed that the experimental results can be interpreted in terms of either of them, because the barriers for the associative pathways are similar to those of the dissociative pathways; thus an enzyme active site could select either of these mechanisms depending on the particular electrostatic environment. From our analysis of the charges we found that the three cations, Ca^{2+}, Mg^{2+} and Zn^{2+}, produce very similar electronic distributions on the dianionic complexes and thus would promote similar reaction paths. This is in agreement with various experimental studies on *Rhodospirillum rubrum* chromatophores showing that the ATPase complex can catalyze Ca-ATP hydrolysis [51-53], albeit with different kinetics than Mg-ATP. Thus, we can confidently assert that the main difference in the biochemical roles of Ca^{2+}, Mg^{2+} and Zn^{2+} in their interactions with pyrophosphates stem from their distinctly different coordination properties.

Because the data presented in this work do not consider the association of the metaphosphate with a nucleophile, they cannot discriminate how associative or dissociative the mechanism of hydrolysis should be; what they show is the feasibility of a partly dissociative path, and the stabilization of a hydroxide anion that can act as a nucleophile stronger than a water molecule, in agreement with the proposal in Ref. [14].

Therefore, in this work we have found evidence of the relevance of the intermolecular interactions in the energetics of pyrophosphate hydrolysis. The facts that hydrated Ca^{2+} is bigger and has a lower oxidizing power than both Mg^{2+} and Zn^{2+} may also provide an explanation to the observation [15] that the former cannot activate the hydrolysis of pyrophosphates chelated to tripositive ions by the membrane-bound pyrophosphatase of *Rhodospirillum rubrum* whereas the two latter do. Nevertheless, a recent study [54] of the soluble *Rhodospirillum rubrum* F1-ATPase showed that unisite hydrolysis in presence of Ca^{2+} is many-fold higher than with Mg^{2+}. The previous hypothesis cannot explain this phenomenon as yet. However it is worth noticing that ATP has three phosphates, thus a different structure, and the active sites of ATPases are bigger than those of PPi-ases [20]. Further studies are required to clarify this.

Acknowledgments

This research was supported by the NSF, U. S. A.-CONACyT, Mexico, Cooperative Science Program, Grant INT-931326, by DGAPA-UNAM, Grant ES-112896 and by CONACyT, Grant L004-E. H. S.-M. Wishes to thank the Mexico-U. S. A. Foundation for Science for a fellowship that allowed him a ten-week stay at U. of A.

Supporting Information Available

Tables listing the cartesian coordinates of all the structures shown in this paper, referred to their respective PMI frames, with their SCF//SCF and MP2//SCF energies. This material can be obtained by request [55] to humberto@fis.unam.mx.

References

1. van Veggel, F. C. J. M.; Verboom, W.; Reinhoudt, D. N. *Chem. Rev*. **1994**, *94*, 280-299.
2. George, P.; Witonski, R. J.; Trachtman, M.; Wu, C.; Dorwart, W.; Richman, L.; Richman, W.; Shurayh, F.; Lentz, B. *Biochim. Biophys. Acta* **1970**, *223*, 1-15.
3. De Meis, L. *Biochim. Biophys. Acta* **1989**, *923*, 333-349.
4. De Meis, L. *Archives Biochem. Biophys.* **1993**, *306*, 287-296.
5. Saint-Martin, H.; Ortega-Blake, I.; Les, A.; Adamowicz, L. *Biochim. Biophys. Acta* **1991**, *1080*, 205-214.
6. Saint-Martin, H.; Ortega-Blake, I.; Les, A.; Adamowicz, L. *Biochim. Biophys. Acta* **1994**, *1207*, 12-23, and references therein.
7. Ma, B.; Meredith, C.; Schaefer III, H. F. *J. Phys. Chem.* **1994**, *98*, 8216-8223.

8. Colvin, M. E.; Evleth, E.; Akacem, Y. *J. Am. Chem. Soc*. **1995**, *117*, 4357-4362.
9. Celis, H.; Romero, I. *J. Bioenerget. Biomembr*. **1987**, *19*, 255-272.
10. Knight, W. B.; Fitts, S. W.; Dunaway-Mariano, D. *Biochemistry* **1981**, *20*, 4079-4086.
11. Ting, S. J.; Dunaway-Mariano, D. *FEBS Lett*. **1984**, *165*, 251-253.
12. Shorter, A. L.; Haromy, T. P.; Scalzo-Brush, T.; Knight, W. B.; Dunaway-Mariano, D.; Sundaralingham, M. *Biochemistry* **1987**, *26*, 2060-2066.
13. Geue, R. J.; Sargeson, A. M.; Wijsekera, R. *Aust. J. Chem.* **1993**, *46*, 1021-1040.
14. Heikinheimo, P.; Lehtonen, J.; Baykov, A.; Lahti, R.; Cooperman, B. S.; Goldman, A. *Structure* **1996**, *4*, 1491-1508.
15. Velázquez, I.; Celis, H.; Romero, I. *BioMetals* **1993**, *6*, 143-148.
16. Westheimer, F. H. *Science* **1987**, *235*, 1173-1178.
17. Taylor, M. G.; Greaves, G. N.; Simkiss, K. *Eur. J. Biochem.* **1990**, *192*, 783-789.
18. Admiraal, S. J.; Herschlag, D. *Chem. Biol*. **1995**, *2*, 729-739.
19. Maegley, K. A.; Admiraal, S. J.; Herschlag, D. *Proc. Natl. Acad. Sci. USA* **1996**, *93*, 8160-8166.
20. Xu, Y.-W.; Moréra, S.; Janin, J.; Cherfils, J. *Proc. Natl. Acad. Sci. USA* **1997**, *94*, 3579-3583.
21. Schlichting, I.; Reinstein, J. *Biochemistry* **1997**, *36*, 9290-9296.
22. Bazzicalupi, C.; Bencini, A.; Bianchi, A.; Cecchi, M.; Escuder, B.; Fusi, V.; García-España, E.; Giorgi, C.; Luis, S. V.; Maccagni, G.; Marcelino, V.; Paoletti, P.; Valtancoli, B. *J. Am. Chem. Soc.* **1999**, *121*, 6807-6815.
23. Huang, C.-C.; Hightower, K. E.; Fierke, C. A. *Biochemistry* **2000**, *39*, 2593-2602.
24. Hayes, M. D.; Kenyon, L. G.; Kollman, P. A. *J. Am. Chem. Soc.* **1978**, *100*, 4331-4340.
25. O'Keeffe, M.; Domengès, B.; Gibbs, G. V. *J. Phys. Chem.* **1985**, *89*, 2304-2309.
26. Ewig, C. S.; van Wazer, J. R. *J. Am. Chem. Soc.* **1988**, *110*, 79-86.
27. Ma, B.; Meredith, C.; Schaefer III, H. F. *J. Phys. Chem.* **1995**, *99*, 3815-3822.
28. Saint-Martin, H.; Ruiz-Vicent, L. E.; Ramírez-Solís, A.; Ortega-Blake, I. *J. Am. Chem. Soc.* **1996**, *118*, 12167-12173.
29. Saint-Martin, H.; Vicent, L. E. *J. Phys. Chem. A* **1999**, *103*, 6862-6872.
30. McCarthy, W. J.; Smith, D. A. M.; Adamowicz, L.; Saint-Martin, H.; Ortega-Blake, I. *J. Am. Chem. Soc.* **1998**, *120*, 6113-6120.
31. Wesolowski, S. S.; Valeev, E. F.; King, R. A.; Baranovski, V.; Schaefer, H. F. III *Mol. Phys.* **2000**, *98*, 1227-1231.
32. Cossi, M.; Barone, V.; Cammi, R.; Tomasi, J. *Chem. Phys. Lett.* **1996**, *255*, 327-335.
33. Frisch, M. J.; Trucks, G. W.; Schlegel, H. B.; Scuseria, G. E.; Robb, M. A.; Cheeseman, J. R.; Zakrzewski, V. G.; Montgomery, J. A. Jr.; Stratmann, R. E.; Burant, J. C.; Dapprich, S.; Millam, J. M.; Daniels, A. D.; Kudin, K. N.; Strain, M. C.; Farkas, O.; Tomasi, J.; Barone, V.; Cossi, M.; Cammi, R.; Mennucci, B.; Pomelli, C.; Adamo, C.; Clifford, S.; Ochterski, J.; Petersson, G. A.; Ayala, P. Y.; Cui, Q.; Morokuma, K.; Malick, D. K.; Rabuck, A. D.; Raghavachari, K.; Foresman, J. B.; Cioslowski, J.; Ortiz, J. V.; Baboul, A. G.; Stefanov, B. B.; Liu, G.; Liashenko, A.; Piskorz, P.; Komaromi, I.; Gomperts, R.; Martin, R. L.; Fox, D. J.; Keith, T.; Al-Laham, M. A.; Peng, C. Y.; Nanayakkara, A.; Gonzalez, C.; Challacombe, M.; Gill, P. M. W.; Johnson, B. G.; Chen, W.; Wong, M. W.; Andres, J. L.; Gonzalez, C.; Head-Gordon, M.; Replogle, E. S.; Pople, J. A., Gaussian 98, Revision A.7, Gaussian, Inc., Pittsburgh PA, **1998**.
34. Rassolov, V.; Pople, J. A.; Ratner, M.; Windus, T. L. *J. Chem. Phys*. **1998**, *109*, 1223.
35. (a) Hehre, W. J.; Ditchfield, R.; Pople, J. A. *J. Chem. Phys.* **1972**, *56*, 2257. (b) Francl, M. M.; Petro, W.J.; Hehre, W. J.; Binkley, J. S.; Gordon, M. S.; DeFrees D. J.; Pople, J. A. *J. Chem. Phys.* **1982**, *77*, 3654.
36. The Extensible Computational Chemistry Environment Basis Set Database, Version 1.0, has been developed and distributed by the Molecular Science Computing Facility, Environmental and Molecular Sciences Laboratory which is part of the Pacific Northwest Laboratory, P.O. Box 999, Richland, Washington 99352, USA, and is funded by the U.S. Department of Energy. The Pacific Northwest Laboratory is a multi-program laboratory operated by Battelle Memorial Institute for the U.S. Department of Energy under contract DE-AC06-76RLO 1830. Contact David Feller, Karen Schuchardt, or Don Jones for further information.
37. Hehre, W. J.; Radom, L.; v. R. Schleyer, P.; Pople, J. A. *Ab Initio Molecular Orbital Theory*, John Wiley & Sons: New York, **1986**; pp. 25, 86, 226, 253.
38. Mulliken, R. S. *J. Chem. Phys.* **1955**, *23*, 1833-1840.
39. Breneman, C. M.; Wiberg, K. B. *J. Comput. Chem.* **1990**, *11*, 361-373.
40. Bernal-Uruchurtu, M. I.; Ortega-Blake, I. *J. Chem. Phys.* **1995**, *103*, 1588-1598.
41. Bernal-Uruchurtu, M. I.; Hernández-Cobos, J.; Ortega-Blake, I. *J. Chem. Phys.* **1998**, *108*, 1750-1751.
42. Bader, R. F. W. *Atoms in Molecules: A Quantum Theory*, Oxford Univ. Press: Oxford, **1990**.
43. Chirlian, L. E.; Francl, M. M. *J. Comput. Chem.* **1987**, *8*, 894-905.
44. Bondi, A. *J. Phys. Chem.* **1964**, *68*, 441-451.
45. Dewar, M. J. S.; Storch, D. M. *Proc. Natl. Acad. Sci. USA* **1985**, *82*, 2225-2229.
46. Warshel, A.; Åqvist, J.; Creighton, S. *Proc. Natl. Acad. Sci. USA* **1989**, *86*, 5820-5824.
47. Celis, H. Private communication.
48. Marcus, Y. *Ion Solvation*, John Wiley and Sons Ltd.: London, **1985**.
49. Florián, J.; Warshel, A. *J. Am. Chem. Soc*. **1997**, *119*, 5473-5474.
50. Florián, J.; Warshel, A. *J. Phys. Chem. B* **1998**, *102*, 719-734.
51. Montero-Lomelí, M.; Dreyfus, G. *Archives Biochem. Biophys.* **1987**, *257*, 345-351.
52. Gromet-Elhanan, Z.; Weiss, S. *Biochemistry* **1989**, *28*, 3645-3650.
53. Montero-Lomelí, M.; Martins, O. B.; Dreyfus, G. *J. Biol. Chem.* **1989**, *264*, 21014--21017.
54. Maldonado, E.; Dreyfus, G.; García, J. J.; Gómez-Puyou, A.; Tuena de Gómez-Puyou, M. *Biochim. Biophys. Acta* **1998**, *1363*, 70-78.
55. Saint-Martin, H. *Technical Report BP-02-98*, **1998**, Centro de Ciencias Físicas, UNAM. Available upon request via E-mail: humberto@fis.unam.mx.